

Dressed-resonance representation for strong photoexcitation of continuum states with application to laser-enhanced autoionization

D. Agassi

Naval Surface Weapons Center, Silver Spring, Maryland 20903-5000

J. H. Eberly

Department of Physics and Astronomy, University of Rochester, Rochester, New York 14627

(Received 28 January 1986)

We introduce in the context of a simple soluble model for laser-enhanced autoionization a new representation—the dressed-resonance representation (DRR). The model includes one autoionizing state, one flat electron continuum, one continuous driving laser of arbitrary strength, and two types of relaxations, i.e., spontaneous decay of the continuum and autoionizing state back to the initial state (spontaneous recycling) and phase-jitter noise in the driving laser. The DRR is a natural extension of the dressed-states representation, employed in strong-field discrete-discrete transitions, to discrete-continuum transitions. We focus on two observables, i.e., the temporal initial state population and the photoelectron spectrum. The emphasis is on strong-field effects. The DRR yields simple, transparent, analytical expressions for the above observables in the no-relaxations limit of the model. These results are complemented by a systematic analysis of the exact solution in all qualitatively distinct physical regimes.

I. INTRODUCTION

The study of strong laser excitation of continuum transitions is rapidly becoming more intensive. New phenomena such as laser embedding of bound states in the electron continuum,¹ multiple-photon absorption above the ionization threshold,² and the production of multiply charged ions by a single laser pulse³ have all been reported. These phenomena have also been discussed separately in a large number of theoretical papers. The theoretical difficulties posed by the action of strong laser light on atoms are manifold, and it is obvious that detailed agreement between theory and experiment over a broad front cannot be expected soon.

In this paper we concentrate on one aspect of these studies with two goals in mind. We consider the problem of photoionization in the case of more than one channel from a bound initial state to the electron continuum. This is in fact the usual case, and is applicable to every atom except hydrogen, for which ionization is inevitably a one-electron process. In every other atom photoionization can be direct or indirect, with the indirect channel involving an autoionizing multielectron discrete state embedded in the continuum above the one-electron ionization threshold. Our goals will be to give as complete a description as possible of the simplest strong-field autoionization process, and at the same time to extend to continuum transitions the usefulness of the dressed-state method. As we will show, this requires the introduction of dressed resonances.

A number of recent theoretical papers¹⁻¹⁰ have treated aspects of strong-field photoinduced autoionization. It has been emphasized that in the strong-field regime one must be concerned with several effects which are not normally important. For example, radiative recombination

can occur fully coherently. That is, the recapture of a positive-energy electron back into a bound state can be induced so quickly that the electron has significant phase memory of the field that originally excited it. Novel features such as strong-field line narrowing of the emitted photoelectron energy spectrum and population trapping in the initial state have been predicted.¹⁻²

Relaxation-assisted transitions have also been studied in such systems, and new features have been predicted for two qualitatively different, common, relaxation processes. These are phase jitter in the driving laser field and spontaneous decay of both the continuum and the autoionizing state back to the initial state (spontaneous recycling). For very rapid phase-jitter relaxation, the photoelectron emission spectrum exhibits a “redistribution” of the line shape which becomes the Fano profile,⁴⁻⁵ normally seen only in absorption. For high spontaneous recycling rates there is a characteristic line narrowing of the “elastic” electron peak.⁴⁻⁵ This latter line narrowing is of different physical origin from the narrowing associated with stimulated transitions.

The present work focuses on the photoelectron spectrum and temporal behavior of the initial state population in a model which includes both strongly stimulated transitions and the two relaxation processes mentioned above. It complements previous work in two respects: (a) We introduce a new representation,⁵ in terms of which the central equations of motion simplify substantially and the results in the semiclassical limit of the model^{1,2} become particularly transparent. This representation is dubbed the dressed-resonance representation (DRR) to underscore its affinity with the dressed-states representation frequently used in conjunction with strongly stimulated discrete-discrete transitions.^{11,12} (b) We present a unified discussion of all qualitatively different regimes in the parameter

space of the model. In so doing previous results and new results are brought into perspective.

The DRR is introduced in the context of a simple model [see Fig. 1(a)] containing an initial state $|0\rangle$, one autoionizing state $|1\rangle$, and one electron-states continuum $|\omega\rangle$. The system, initially in $|0\rangle$, is driven by one continuous laser of arbitrary strength. The gist of the DRR is schematically displayed in Fig. 2. In the absence of a continuum, the stimulated transitions between $|0\rangle$ and $|1\rangle$ give rise to the two dressed states $|d_0\rangle$ and $|d_1\rangle$ [Figs. 2(b) and 2(c)]. Due to the coupling of $|d_0\rangle$ and $|d_1\rangle$ to the continuum both by stimulated transitions and static coupling, they transform into resonances, i.e., the dressed resonances [Fig. 2(d)]. This admixing is also referred to as embedding. We readily recognize [Fig. 2(c)] that the present embedding is of the same type first studied by Fano,¹³ involving, however, two bound states. Hence it has a simple analytical solution. Thus the new feature of the DRR is that the stimulated transitions are *completely* diagonalized from the outset. The resulting perturbed continuum states pertaining to frequency ω_0 , namely the DRR basis states $|\tilde{\omega}_0\rangle$, have therefore the expansion

$$|\tilde{\omega}_0\rangle = a_0(\omega_0)|d_0\rangle + a_1(\omega_0)|d_1\rangle + \int d\omega b_\omega(\omega_0)|\omega\rangle, \quad (1.1)$$

with explicitly known coefficients [Sec. IV]. The frequency dependence of $a_0(\omega_0)$ and $a_1(\omega_0)$ shows a two-peaked line shape which reflects the two underlying dressed resonances.

The simplifying feature of the DRR is best demonstrated by the expressions for the photoelectron spectrum $S(\omega)$ and the population of the initial state $P_0(t)$ in the limit of no relaxations (Sec. IV),

$$S(\omega) = |\langle 0|\tilde{\omega}\rangle|^2, \quad (1.2)$$

$$P_0(t) = \left| \int d\omega e^{-i\omega t} S(\omega) \right|^2.$$

Given expansion (1.1), expressions (1.2) expose the role

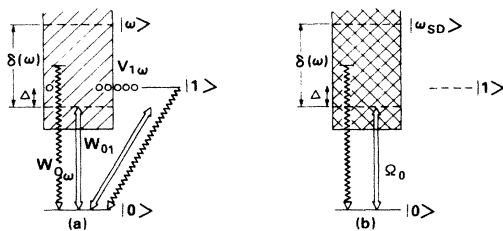


FIG. 1. Schematic representation of the model space and couplings in (a) the unperturbed representation and (b) the semiclassical dressed representation (SDR). The states $|0\rangle$, $|1\rangle$ denote the initial and autoionizing states, respectively, and the hatched area represents the single-electron continuum. The two-way double arrow and one-way wavy arrow denote stimulated and spontaneous-decay transitions, respectively. The relevant detunings $\Delta, \delta(\omega)$, the discrete-continuum couplings $W_{0\omega}$ and Ω_0 , the discrete-discrete coupling W_{01} , and the static autoionizing state-continuum coupling $V_{1\omega}$ are defined in the text.

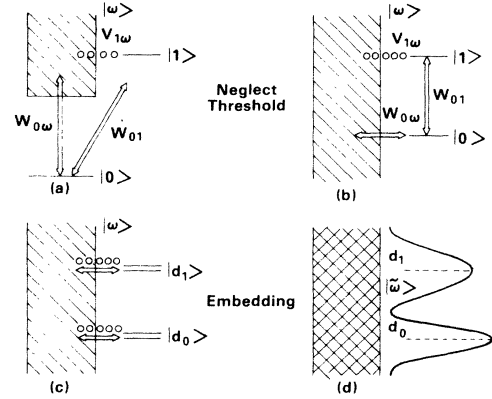


FIG. 2. Origin of the dressed resonance representation (DRR). Starting from the unperturbed representation (a), the equivalent model space in which the continuum threshold is neglected is depicted in (b). (c) represents the basis after diagonalizing the discrete-discrete coupling thereby generating the dressed states $|d_0\rangle, |d_1\rangle$. The full diagonalization (d) gives rise to the DRR continuum $|\tilde{\omega}\rangle$. Its dipole strength distribution manifests a two-hump ω dependence reflecting the two dressed states in the model.

of the dressed resonances in determining the line shapes (location and width) of $S(\omega)$ and the oscillatory-decaying behavior of $P_0(t)$. To appreciate these simple expressions they should be compared to an equivalent treatment in another representation²⁻³ (the semiclassical dressed representation, see below). Unfortunately no counterparts to (1.2) exist in the presence of recycling and phase-jitter relaxations except in limiting cases⁴ (Sec. V). Although the equations of motion simplify considerably in the DRR, they cannot be solved in a closed form. We therefore discuss their content by combining numerical examples and qualitative arguments within the DRR framework.

The paper is organized as follows. The model is defined in the unperturbed representation [Fig. 1(a)] in Sec. II, and the central equations of motion in the DRR are derived in Sec. III. Section IV is devoted to establishing the details of the DRR and examining the semiclassical limit of the model for which simple expressions exist, such as those given in Eq. (1.2). Hereafter the term "semiclassical" implies that we treat the laser field classically (as a c number) and the atom and all spontaneous photons quantum mechanically. Two analytic results pertaining to the full model, i.e., with relaxations, are given in Sec. V. Section VI is a systematic qualitative analysis of the various regimes in the physical parameter space of the model. The discussion is substantiated by representative examples of exact numerical solutions of the model. The conclusions are given in Sec. VI. The Appendixes contain technical details.

II. THE MODEL

The model is introduced in the unperturbed representation, Fig. 1(a). The model space is comprised of the initial state $|0\rangle$, one autoionizing state $|1\rangle$, one flat (constant dipole strength distribution) continuum of states $|\omega\rangle$, and one laser field of arbitrary strength. The laser field is

continuous after being turned on abruptly at $t=0$.

The model Hamiltonian (carets hereafter denote operators) is of the form

$$\hat{H} = \hat{H}_A + \hat{H}_R + \hat{H}_{\text{int}}. \quad (2.1)$$

The single-atom Hamiltonian \hat{H}_A is¹⁻⁷

$$\hat{H}_A = E_0 |0\rangle\langle 0| + E_1 |1\rangle\langle 1| + \int d\omega \hbar\omega |\omega\rangle\langle \omega| + \int d\omega \hbar V_{1\omega} (|1\rangle\langle \omega| + |\omega\rangle\langle 1|), \quad (2.2)$$

where the continuum states are δ normalized: $\langle \omega | \omega' \rangle = \delta(\omega - \omega')$, and the static $V_{1\omega}$ interaction is real and assumed to be ω independent. The quantized free-radiation Hamiltonian \hat{H}_R has the standard form¹⁴

$$\hat{H}_R = \sum_{\lambda} \hbar\omega_{\lambda} \hat{a}_{\lambda}^{\dagger} \hat{a}_{\lambda}, \quad (2.3)$$

where $\lambda = [\mathbf{k}, \epsilon_s]$, $s = 1, 2$ labels the field eigenmodes in a box of volume V . Each mode is characterized by a momentum \mathbf{k} and a polarization vector ϵ_s which assumes two orthogonal transverse directions. The associated creation and annihilation operators are $\hat{a}_{\lambda}^{\dagger}, \hat{a}_{\lambda}$ respectively and $\omega_{\lambda} = ck$.

The interaction Hamiltonian \hat{H}_{int} in the dipole and rotating-wave approximation is²⁻⁶

$$\begin{aligned} \hat{H}_{\text{int}} &= \sum_{\lambda} [\hbar\Omega_{\lambda}^*(1) \hat{B}^{\dagger}(1) \hat{a}_{\lambda} + \text{H.c.}] \\ &+ \sum_{\lambda} \int d\omega [\hbar\Omega_{\lambda}^*(\omega) \hat{B}^{\dagger}(\omega) \hat{a}_{\lambda} + \text{H.c.}] \\ &= \sum_{\lambda} \sum_j [\hbar\Omega_{\lambda}^*(j) \hat{B}^{\dagger}(j) \hat{a}_{\lambda} + \text{H.c.}], \end{aligned} \quad (2.4)$$

where the transition dipole operator $\hat{B}(j)$ is defined by

$$\hat{B}(j) = |0\rangle\langle j| \quad \text{for } |j\rangle = |1\rangle, |\omega\rangle \quad (2.5)$$

and the coupling constant $\Omega_{\lambda}(j)$ is given by

$$\begin{aligned} \Omega_{\lambda}(j) &= -ig_{\lambda} V_{0j}, \\ V_{0j} &= |e| \langle 0 | \mathbf{r} | j \rangle (\omega_j - \omega_0) / \hbar c, \\ g_{\lambda} &= \left[\frac{2\pi\hbar c^2}{\omega_{\lambda} V} \right]^{1/2} (\mathbf{n}_r \cdot \epsilon_s). \end{aligned} \quad (2.6)$$

The form (2.4)–(2.6) is derived from the $\mathbf{A} \cdot \mathbf{p}$ interaction term. The new symbols in (2.6) are \mathbf{n}_r , a unit vector such that $\langle 0 | \mathbf{r} | j \rangle = \langle 0 | \mathbf{r} | j \rangle \mathbf{n}_r$, $|e|$ is the electric charge in Gaussian units, and $E_j = \hbar\omega_j$, $j = 1, \omega$. Hereafter summa-

tion or labeling by j refers jointly to the autoionizing state $|1\rangle$ and continuum $|\omega\rangle$ as in (2.4)–(2.6). We assume throughout that the coupling strengths V_{0j} are constants, in keeping with a similar assumption made earlier on $V_{1\omega}$. These constants are treated as free parameters of the model. In practice their value depends on the particular atom and the specific structure of the autoionizing state.¹⁵

The model (2.4) has also been considered in a representation in which the $|1\rangle$ - $|\omega\rangle$ coupling of Eq. (2.2) has been prediagonalized as indicated by Fig. 1(b).^{2,6} This representation is hereafter referred to as the semidressed representation (SDR) since it implies the embedding of only *one* state (the autoionizing state). This should be compared to the embedding of two states (the initial and autoionizing states) underlying the DRR (Fig. 2) and the embedding of no states in the unperturbed representation as in Fig. 1(a). The equations of motion pertaining to the model in the SDR are elaborated in several Appendixes. A central factor in these equations is the Fano profile¹³ which is the dipole strength distribution [analogue of $\Omega_{\lambda}(j)$ in Eq. (2.6)] for transitions between $|0\rangle$ and the SDR continuum states. The relation between the physical parameters in the unperturbed representation, in the DRR, and the Fano profile are given in Sec. III.

III. THE EQUATIONS OF MOTION IN THE DRR

To solve for the photoelectron spectrum and initial state population—the atomic observables at the focus of this work—we need the initial density matrix and the Heisenberg equation of motion for a general atomic operator $\hat{O}_A(t)$, which eventually is chosen to be a member of a convenient complete set of atomic operators. As is shown below, the model suggests a natural choice for a complete set $\hat{O}_A(t)$ and the corresponding representation, i.e., the DRR.

The starting point is the Heisenberg equation of motion for a general atomic operator $\hat{O}_A(t)$ in the unperturbed representation. After eliminating the radiation field degrees of freedom using the Markov approximation (Appendix A and Refs. 5, 14, 16, and 17) the equation of motion is

$$\begin{aligned} i\hbar \frac{d}{dt} (\hat{O}_A(t))_H &= i\hbar \left[\frac{\partial}{\partial t} \hat{O}_A(t) \right]_H \\ &+ \hbar \hat{S}_{\text{stm}}(t) + \hbar \hat{S}_{\text{spn}}(t), \end{aligned} \quad (3.1)$$

where the source terms for the stimulated and spontaneous transitions are denoted by $\hat{S}_{\text{stm}}(t)$, and $\hat{S}_{\text{spn}}(t)$, respectively, and given by

$$\begin{aligned} \begin{bmatrix} \hbar \hat{S}_{\text{stm}}(t) \\ \hbar \hat{S}_{\text{spn}}(t) \end{bmatrix} &= \begin{bmatrix} ([\hat{O}_A(t), \hat{H}_A])_H \\ 0 \end{bmatrix} + \sum_{\lambda, j} \left[\hbar \Omega_{\lambda}^*(j) ([\hat{O}_A(t), \hat{B}^{\dagger}(j)])_H \begin{bmatrix} \hat{a}_{\lambda}^{(v)}(t) \\ \hat{a}_{\lambda}^{(s)}(t) \end{bmatrix} \right. \\ &\quad \left. + \hbar \Omega_{\lambda}(j) \begin{bmatrix} [\hat{a}_{\lambda}^{(v)}(t)]^{\dagger} \\ [\hat{a}_{\lambda}^{(s)}(t)]^{\dagger} \end{bmatrix} ([\hat{O}_A(t), \hat{B}(j)])_H \right], \end{aligned} \quad (3.2a)$$

where $\hat{a}_\lambda^{(v)}(t)$ is the "vacuum" radiation field operator defined below, $\hat{a}_\lambda^{(s)}$ is the source field operator,

$$\hat{a}_\lambda^{(s)}(t) = -i\pi \sum_j \Omega_\lambda(j) \delta(\omega_\lambda - \omega_j) (\hat{B}(j))_H, \quad (3.2b)$$

and the parenthesis $()_H$ indicates the Heisenberg representation evaluated at time t .

To evaluate the interesting atomic observables it will be required to consider the expectation value of (3.1) with regard to the initial density matrix. As stated in Sec. II, the atom is initially at the state $|0\rangle$. The initial state of the radiation field $|\alpha\rangle$ is assumed to be a coherent state,¹⁸

$$\hat{a}_\lambda^{(v)}(t) |\alpha\rangle = \delta_{\lambda,L} \alpha e^{-i[\omega_L t + \psi(t)]} |\alpha\rangle, \quad (3.3)$$

where L denotes the mode (wave vector and polarization) of the driving laser field, ω_L its frequency, and $\psi(t)$ is a stochastic phase satisfying

$$\langle \dot{\psi}(t) \dot{\psi}(t') \rangle = 2\gamma_T \delta(t - t'), \quad (3.4)$$

and $\langle \rangle$ denotes an ensemble average.^{2,4,5,19} The eigenvalue α measures the strength of the driving laser field and $\langle \alpha | \mathbf{E}(t) | \alpha \rangle$ is the semiclassical expression for the laser's electric field.²⁰ In the absence of phase jitter Eq. (3.3) expresses the standard initial condition representing a continuous classical laser field by a coherent state $|\alpha\rangle$. In the presence of phase jitter, the parameter γ_T can be identified as the laser's half bandwidth. Equation (3.3) is a simple way to incorporate in the present framework classical noise pertaining to the driving laser.

To clarify the meaning of (3.1) we examine first the $S_{\text{stim}}(t)$ source term, which represents the stimulated transitions' effect. This interpretation of $S_{\text{stim}}(t)$ is based on the following consideration. Since only atomic expectation values of the form $\langle \alpha | (\hat{O}_A(t))_H | \alpha \rangle$ are needed, it follows from (3.2) and (3.3) that

$$\begin{aligned} \langle \alpha | \hbar \hat{S}_{\text{stim}}(t) | \alpha \rangle &= \langle \alpha | [(\hat{O}_A(t), \hat{H}_{\text{SC}}^{(0)}(t))]_H | \alpha \rangle \\ \hat{H}_{\text{SC}}^{(0)}(t) &= \hat{H}_A + \sum_j [\hbar \Omega_L^*(j) \alpha \hat{B}^\dagger(j) e^{-i[\omega_L t + \psi(t)]} + \text{H.c.}] \end{aligned} \quad (3.5)$$

Hence $S_{\text{stim}}(t)$ is a commutator with the Hamiltonian which describes the stimulated transitions in the model, i.e., this term represents the stimulated-transition-induced

rate of change.

To simplify (3.5) it is transformed to the rotating frame

$$\hat{H}_{\text{SC}}^{(0)}(t) = \hat{R}_0(t) \hbar \hat{h}_{\text{SC}}^{(0)} \hat{R}_0^\dagger(t), \quad (3.6)$$

where $\hat{R}_0(t), \hat{h}_{\text{SC}}^{(0)}$ are given in Appendix B. Therefore, for the choice

$$\hat{O}_A(t) = \hat{R}_0(t) \hat{O}_A \hat{R}_0^\dagger(t) \quad (3.7)$$

with \hat{O}_A still unspecified, the equation of motion (3.1) (set $\hat{S}_{\text{spn}}(t) = 0$ for the moment) takes the form

$$\begin{aligned} \frac{d}{dt} \langle \alpha | (\hat{O}_A(t))_H | \alpha \rangle &= -i \langle \alpha | (\hat{R}_0(t) [\hat{O}_A, \hat{h}_{\text{SC}}] \hat{R}_0^\dagger(t))_H | \alpha \rangle \\ &\quad - i \dot{\psi}(t) \langle \alpha | (\hat{R}_0(t) [\hat{O}_A, |0\rangle\langle 0|] \hat{R}_0^\dagger(t))_H | \alpha \rangle. \end{aligned} \quad (3.8)$$

In deriving (3.8) we used the explicit form of $\hat{R}_0(t)$, given in Eq. (B1). The full semiclassical Hamiltonian in the rotating frame \hat{h}_{SC} is

$$\begin{aligned} \hbar \hat{h}_{\text{SC}} &= \hbar \hat{h}_A + \sum_j \hbar W_{0j} [\hat{B}^\dagger(j) + \hat{B}(j)], \\ \hbar \hat{h}_A &= \hat{H}_A + \hbar \omega_L |0\rangle\langle 0| - (E_0 + \hbar \omega_L) \hat{1} \\ &= \hbar \Delta |1\rangle\langle 1| + \int d\omega \hbar \delta(\omega) |\omega\rangle\langle \omega|, \end{aligned} \quad (3.9)$$

where

$$\begin{aligned} \Delta &= \omega_1 - \omega_L, \\ \delta(\omega) &= \omega - \omega_L, \\ W_{0j} &= \Omega_L^*(j) \alpha, \end{aligned} \quad (3.10)$$

and $E_0 = 0$ henceforth. Combining (2.6) with (3.10) it follows that $W_{0j} = \langle 0 | \{ \langle \alpha | \mathbf{E} | \alpha \rangle \cdot \mathbf{d} \} | j \rangle / \hbar$ where \mathbf{d} is the dipole moment. Notice that the \hbar 's have now been placed so that all important parameters and operators have frequency units.

The last step is to carry out the ensemble average of (3.8), given the statistical assumptions of (3.4). By virtue of a well-known theorem which applies to white-noise multiplicative stochastic processes²¹ it follows that

$$\begin{aligned} \frac{d}{dt} \langle \langle \alpha | (\hat{R}_0(t) \hat{O}_A \hat{R}_0^\dagger(t))_H | \alpha \rangle \rangle &= -i \langle \langle \alpha | (\hat{R}_0(t) [\hat{O}_A, \hat{h}_{\text{SC}}] \hat{R}_0^\dagger(t))_H | \alpha \rangle \rangle \\ &\quad - \gamma_T \langle \langle \alpha | (\hat{R}_0(t) [\hat{O}_A, |0\rangle\langle 0|] |0\rangle\langle 0| \hat{R}_0^\dagger(t))_H | \alpha \rangle \rangle, \end{aligned} \quad (3.11)$$

where the brackets $\langle \rangle$ indicate an average over the ensemble of laser phase fluctuations.

Equation (3.11) offers a natural starting point to introduce the DRR and exposes the dilemma in choosing a representation convenient for treating both the stimulated and phase-jitter-assisted transitions. When stimulated transitions are dominant an obvious choice of representation and complete set of operators \hat{O}_A is such that the first term in the right-hand side (RHS) of (3.11) simplifies. This representation is the DRR defined by

$$\hat{h}_{\text{SC}} | \tilde{\omega} \rangle = \delta(\omega) | \tilde{\omega} \rangle \quad (3.12)$$

and a corresponding convenient complete set of operators is

$$\hat{O}_A = \{ |\tilde{\omega}\rangle \langle \tilde{\omega}'| \}, \text{ for all } \omega, \omega'. \quad (3.13)$$

The representation (3.12), not surprisingly, is not optimal with respect to the γ_T term in (3.11). The latter term is particularly simple in the SDR and unperturbed representations (since in both of them the state $|0\rangle$ is a member of the basis), combined with the choice $\hat{O}_A = \{ |a\rangle \langle b| \}$ where $|a\rangle, |b\rangle$ are states of the basis. In this work we pursue the DRR since the simplification gained in the first RHS term of (3.11) more than compensates for the added complexity of the γ_T term. The numerical calculations, however, have been carried out in the SDR.

The $\hat{S}_{\text{spn}}(t)$ term in (3.1) describes recycling-assisted transitions. This can be inferred from (3.2) since $\hat{a}_\lambda^{(s)}$ describes self-reaction contributions.¹⁶ Using the explicit form of $\hat{R}_0(t)$ and adding $\hat{S}_{\text{spn}}(t)$ to (3.11), the full equations of motion for the amplitudes

$$C(\omega_0, \omega'_0; t) = \langle \langle \alpha | \langle 0 | (\hat{R}_0(t) | \tilde{\omega}_0 \rangle \langle \tilde{\omega}'_0 | \hat{R}_0^\dagger(t))_H | 0 \rangle | \alpha \rangle \rangle \quad (3.14)$$

are

$$\begin{aligned} \frac{d}{dt} C(\omega_0, \omega'_0; t) &= i[\delta(\omega_0) - \delta(\omega'_0)] C(\omega_0, \omega'_0; t) + \langle 0 | \tilde{\omega}_0 \rangle \langle \tilde{\omega}'_0 | 0 \rangle M(t) \\ &\quad - \int d\omega' [C(\omega_0, \omega'; t) R(\omega') F^*(\omega'_0) + F(\omega_0) R^*(\omega') C(\omega', \omega'_0; t)] \\ &\quad - \gamma_T \int d\omega' [C(\omega_0, \omega'; t) r(\omega') r^*(\omega'_0) + r(\omega_0) r^*(\omega') C(\omega', \omega'_0; t)] \end{aligned} \quad (3.15)$$

The new symbols in (3.15) signify the following: $M(t)$ is a linear combination of the unknown amplitudes (3.14) not entering the subsequent discussion and therefore not quoted. It can be explicitly shown that the $M(t)$ term guarantees unitarity, i.e.,

$$\frac{d}{dt} \int d\omega C(\omega, \omega; t) = 0. \quad (3.16)$$

The third term in the RHS of (3.15) corresponds to $\hat{S}_{\text{spn}}(t)$ and represents the recycling-assisted transitions. The ‘‘perturbed Fano profile’’ $F(\omega)$ is given by

$$\begin{aligned} F(\omega_0) &= F_B(\omega_0) + F_C(\omega_0), \\ F_B(\omega_0) &= V_{01} \langle 1 | \tilde{\omega}_0 \rangle, \\ F_C(\omega_0) &= V_{0\omega} \int d\omega \langle \omega | \tilde{\omega}_0 \rangle, \end{aligned} \quad (3.17)$$

and the associated $R(\omega)$ factors are

$$\begin{aligned} R(\omega) &= R_B(\omega) + R_C(\omega) = Q(\omega_1) F(\omega), \\ Q(\omega) &= \pi \sum_\lambda g_\lambda^2 \delta(\omega_\lambda - \omega) = \frac{2}{3} \frac{\hbar\omega}{c}. \end{aligned} \quad (3.18)$$

The expression for $R_C(\omega)$ is approximated. The last term on the RHS of (3.15) obviously represents the phase-jitter-assisted transitions, and

$$r(\omega) = \langle 0 | \tilde{\omega} \rangle. \quad (3.19)$$

Finally, the initial conditions for the amplitudes (3.14) are obviously

$$C(\omega_0, \omega'_0; t=0) = \langle 0 | \tilde{\omega}_0 \rangle \langle \tilde{\omega}'_0 | 0 \rangle. \quad (3.20)$$

The equations of motion (3.15) are the central result of this work. They possess several attractive features: (a) They are substantially simpler than their counterparts in the SDR (Appendix C). This is mainly due to the occurrence of the perturbed Fano profile $F(\omega)$, Eq. (3.17), in comparison to the SDR equations which involve only the

unperturbed Fano profile $F_0(\omega)$ [Eq. (3.23)]. In this way important distortions in the effective dipole strength distribution due to the stimulated transitions are accounted for from the outset. (b) The semiclassical limit of the model,² i.e., $Q(\omega) = \gamma_T = M(t) = 0$ is trivially solved [see Sec. IV]. Consideration of this limit yields explicit expressions for the DRR basis as well as useful insights. (c) Note the similar structure of the recycling and γ_T terms in (3.15) by pairing γ_T with $Q(\omega_1)$ and $F(\omega_0)$ with $r(\omega_0)$. This analogy is somewhat surprising given the very different physical origin of these two noises. This property makes it possible to solve (3.15) exactly using the method employed for solving the equations of motion in the SDR [Appendixes C and D]. (d) The decomposition of (3.17) and (3.18) into ‘‘bound’’ and ‘‘continuum’’ contributions corresponds to the different ‘‘physics’’ at the $q=0$ and $|q|=\infty$ limits where q is the Fano asymmetry parameter defined below in Eq. (3.23). These two qualitatively different regimes [see Sec. VI] are naturally separated in the DRR.

To complete the scheme we now demonstrate the connection between the amplitudes (3.14) and the quantities of interest. Consider first the initial state population $P_0(t)$. By definition, with $\hat{\rho}(t)$ for the full density matrix,

$$\begin{aligned} P_0(t) &= \langle \text{tr}[\hat{\rho}(t) | 0 \rangle \langle 0 |] \rangle \\ &= \langle \text{tr}[\hat{R}(t) \hat{\rho}_0 \hat{R}^\dagger(t) | 0 \rangle \langle 0 |] \rangle \\ &= \langle \text{tr}[\hat{\rho}_0 \hat{R}^\dagger(t) [\hat{R}_0(t) | 0 \rangle \langle 0 | \hat{R}_0^\dagger(t)] \hat{R}(t)] \rangle \\ &= \langle \langle \alpha | \langle 0 | (\hat{R}_0(t) | 0 \rangle \langle 0 | \hat{R}_0^\dagger(t))_H | 0 \rangle | \alpha \rangle \rangle, \end{aligned} \quad (3.21)$$

where $\hat{R}(t)$ is the full evolution operator. In deriving (3.21) we used $[\hat{R}_0(t), |0\rangle\langle 0|] = 0$, Eq. (B1), and the form of the initial density matrix $\hat{\rho}_0 = |0\rangle\langle\alpha| \langle\alpha| \langle 0|$. By the same token the photoelectron spectrum is

$$\begin{aligned}
S(\omega) &= \lim_{t \rightarrow \infty} \langle \text{tr} \{ \hat{\rho}(t) | \omega \rangle \langle \omega | \} \rangle \\
&= \lim_{t \rightarrow \infty} \langle \langle \alpha | \langle 0 | (\hat{R}_0(t) | \omega \rangle \langle \omega | \hat{R}_0^\dagger(t))_H | 0 \rangle | \alpha \rangle \rangle,
\end{aligned} \tag{3.22}$$

since $\hat{R}_0(t)$ is a unit operator in the unperturbed continuum space. Consequently, by invoking the unitary transformation between $|\bar{\omega}\rangle$ and $(|0\rangle, |\omega\rangle)$, it is possible to express $S(\omega)$ and $P_0(t)$ in terms of (3.14) (Sec. IV). Note, however, that for the expectation value of a coherence such as $|0\rangle\langle j|$, an extra phase should be added to (3.21), for example, since $\hat{R}_0(t)|0\rangle\langle j|\hat{R}_0^\dagger(t) = e^{-i\omega_L t}|0\rangle\langle j|$.

To establish a reference with previous work¹⁻⁷ it is instructive to state the relations between the physical parameters in the different representations. In the SDR the Fano profile $F_0(\omega)$ was introduced in the following parametrization:^{2,4}

$$F_0(\omega) = \frac{\Omega_0}{(4\pi\gamma_1)^{1/2}} \left[\frac{\gamma_1}{\omega - \omega_1 + i\gamma_1} - \frac{1}{1+iq} \frac{\sigma}{\omega - \omega_1 + i\sigma} \right], \tag{3.23}$$

$$\gamma_1 = \pi |V_{1\omega}|^2,$$

where $\hbar\omega_1 = E_1 - E_0$, σ is a cutoff parameter set to infinity at the end of the calculation, and q and Ω_0 are the Fano asymmetry and strength parameters, respectively.¹³ Since the effective Hamiltonian (3.9) is identical to the Hamiltonian used in studies where the SDR is employed, we identify²

$$\begin{aligned}
\Omega_0 &= (4\pi\gamma_1)^{1/2} (q+i) W_{0\omega} e^{i\phi}, \\
q &= \frac{W_{01} + \int d\omega V_{1\omega} \frac{P}{\omega_1 - \omega} W_{0\omega}}{\pi W_{0\omega_1} V_{1\omega_1}} \approx \frac{W_{01}}{\pi W_{0\omega} V_{1\omega}}.
\end{aligned} \tag{3.24}$$

Inverting (3.24) for real q and Ω_0 gives

$$\begin{aligned}
W_{01} &= \frac{\Omega_0}{2} \frac{q}{(1+q^2)^{1/2}}, \\
W_{0\omega} &= \frac{\Omega_0}{(4\pi\gamma_1)^{1/2}} \frac{1}{(1+q^2)^{1/2}}.
\end{aligned} \tag{3.25}$$

Combining (3.25), (3.10), and (2.6) establishes the relations between the parameters in the unperturbed representation, the DRR and the SDR.

Finally, we make a choice of a parameter which gauges the recycling frequency. This frequency is obviously related to the factor $Q(\omega_1)$, Eq. (3.18). A more convenient choice, however, is the frequency-dimensioned combination

$$\gamma_S = Q(\omega_1) \left[\frac{\Omega_0}{2} \right]^2 / |\alpha g_{\omega_1}|^2. \tag{3.26}$$

It can be easily verified that in the $q \rightarrow \infty$ limit, when only $F_B(\omega)R_B(\omega)$ contribute to (3.15), γ_S as defined in (3.26) is a prefactor just like γ_T . The γ_S is also a natural

TABLE I. Dimensionality checklist.

Quantity	Dimensionality
$[\hat{B}(1)]$	1
$[\omega\rangle]$	$t^{1/2}$
$[\hat{B}(\omega)]$	$t^{1/2}$
$[g_\lambda]$	$E^{1/2}/l^{1/2}$
$[V_{01}]$	$l^{1/2}/(E^{1/2}t)$
$[V_{0\omega}]$	$l^{1/2}/(E^{1/2}t^{1/2})$
$[V_{1\omega}]$	$1/t^{1/2}$
$[\Omega_0]$	$1/t$
$[\gamma_1]$	$1/t$
$[\alpha g_\lambda]$	$E^{1/2}/l^{1/2}$
$[W_{01}]$	$1/t$
$[W_{0\omega}]$	$1/t^{1/2}$
$[Q(\omega)]$	Et/l
$[F(\omega)]$	$l^{1/2}/E^{1/2}t^{1/2}$
$[R(\omega)][F(\omega)]$	1
γ_S	$1/t$

combination in the SDR equations of motion used for the numerical calculations. Another interpretation of γ_S is as half the Einstein coefficient of the autoionizing resonance. To see that, consider the two-level limit (i.e., $\gamma_1 \rightarrow 0$, $|q| \rightarrow \infty$) of the Fano profile $F_0(\omega)$. Then

$$\int d\omega |F_0(\omega)|^2 = \left[\frac{\Omega_0}{2} \right]^2 = (W_{01})^2 = |V_{01}\alpha g_{\omega_1}|^2, \tag{3.27}$$

where we used (3.10). Inserting the expression for V_{01} from (2.6) it follows that

$$\gamma_S = \frac{A}{2} = \frac{2}{3} \frac{\omega_1^3 |e|^2 |\langle 0|r|1\rangle|^2}{\hbar c^3}, \tag{3.28}$$

where A is the Einstein coefficient.¹⁴ This result is conducive to adopt the same interpretation of γ_S for finite γ_1 and q .

An instructive check of the relations introduced in Secs. II and III is to examine the relevant dimensionality. A dimensionality checklist (Table I) is added for this purpose.

IV. THE SEMICLASSICAL LIMIT

As has been shown in Sec. III, the DRR arises naturally in the context of stimulated transitions to a continuum and yields relatively simple equations of motion. This result is now complemented by demonstrating the simplicity of constructing the DRR basis $|\bar{\omega}\rangle$ and gaining physical insight from examining the semiclassical pure-state limit of the model. This limit has been considered before.^{1,2} The ease of reproducing the known results underscores the usefulness of the DRR.

The semiclassical pure-state limit corresponds to treating the radiation field as a c number and eliminating relaxations, i.e., taking $\gamma_S = \gamma_T = 0$. This is equivalent to starting from the effective Hamiltonian $\hat{H}_{SC}^{(0)}(t)$, given in Eq. (3.5), or its counterpart in the rotating frame \hat{h}_{SC} ,

given in Eq. (3.9). The key remark, graphically depicted in Fig. 2, is that the diagonalization of \hat{h}_{SC} is a Fano-type problem with two bound states and one continuum.¹³ Hence it is easily solved. To demonstrate this we decompose

$$\hat{h}_{\text{SC}} = \hat{h}_B + \hat{h}_C \quad (4.1)$$

with

$$\begin{aligned} \hat{h}_B &= \Delta |1\rangle\langle 1| + W_{01} [|0\rangle\langle 1| + |1\rangle\langle 0|], \\ \hat{h}_C &= \int d\omega \delta(\omega) |\omega\rangle\langle \omega| + \int d\omega V_{1\omega} [|1\rangle\langle \omega| \\ &\quad + |\omega\rangle\langle 1|] + \int d\omega W_{0\omega} [|0\rangle\langle \omega| + |\omega\rangle\langle 0|]. \end{aligned} \quad (4.2)$$

The first step is the diagonalization of \hat{h}_B depicted in the transition from Fig. 2(b) to Fig. 2(c). The eigenfunctions $|d_i\rangle$ are

$$\hat{h}_B |d_i\rangle = \omega_{d_i} |d_i\rangle, \quad i=0,1 \quad (4.3)$$

where

$$\begin{aligned} \begin{bmatrix} |d_0\rangle \\ |d_1\rangle \end{bmatrix} &= \begin{bmatrix} \cos\theta & -\sin\theta \\ \sin\theta & \cos\theta \end{bmatrix} \begin{bmatrix} |0\rangle \\ |1\rangle \end{bmatrix}, \\ \tan 2\theta &= \frac{2W_{01}}{\Delta}, \end{aligned} \quad (4.4)$$

$$\begin{aligned} \omega_{d_0} &= \frac{1}{2} [\Delta - (\Delta^2 + 4W_{01}^2)^{1/2}], \\ \omega_{d_1} &= \frac{1}{2} [\Delta + (\Delta^2 + 4W_{01}^2)^{1/2}]. \end{aligned} \quad (4.5)$$

The $|d_i\rangle$ are the so-called ‘‘dressed states,’’ introduced in conjunction with strong-field discrete-discrete stimulated transitions.^{11,12} No reference to ‘‘number of photons’’ is necessary.

The next step in the diagonalization of \hat{h}_{SC} is to reexpress \hat{h}_C , Eq. (4.2), in terms of the dressed states $|d_i\rangle$ [Fig. 2(c)] and to embed them into the continuum $|\omega\rangle$. At this point the similarity with the Fano problem is obvious: The two bound states to be embedded are the dressed states. The result [Fig. 2(d)] is the dressed resonances and the associated DRR basis $|\tilde{\omega}\rangle$,

$$\hat{h}_{\text{SC}} |\tilde{\omega}\rangle = \delta(\omega) |\tilde{\omega}\rangle \quad (4.6)$$

[see (3.12)], where $|\tilde{\omega}\rangle$ has the following expansion:⁵

$$\begin{aligned} |\tilde{\omega}\rangle &= a_0(\omega_0) |d_0\rangle + a_1(\omega_0) |d_1\rangle + \int d\omega b_\omega(\omega_0) |\omega\rangle, \\ a_i(\omega_0) &= \left[\frac{\tilde{\gamma}_i}{\pi} \right]^{1/2} \frac{[\delta(\omega_0) - \omega_{d_{|i-1|}}]}{p(\omega_0)}, \quad i=0,1 \\ b_\omega(\omega_0) &= \delta(\omega_0 - \omega) + \frac{1}{\omega - \omega_0 + i\eta} \\ &\quad \times \left[1 - \frac{[\delta(\omega_0) - \omega_{d_0}][\delta(\omega_0) - \omega_{d_1}]}{p(\omega_0)} \right] \\ &= \delta(\omega_0 - \omega) + \frac{1}{\omega - \omega_0 + i\eta} \sum_i \left[\frac{\tilde{\gamma}_i}{\pi} \right]^{1/2} a_i(\omega_0). \end{aligned} \quad (4.7)$$

The new symbols in (4.7) are the widths of the dressed

states $\tilde{\gamma}_i$,

$$\begin{aligned} \left[\frac{\tilde{\gamma}_0}{\pi} \right]^{1/2} &= \langle \omega | \hat{h}_{\text{SC}} | d_0 \rangle \\ &= -(\sin\theta) \left[\frac{\gamma_1}{\pi} \right]^{1/2} + (\cos\theta) W_{0\omega} \\ \left[\frac{\tilde{\gamma}_1}{\pi} \right]^{1/2} &= \langle \omega | \hat{h}_{\text{SC}} | d_1 \rangle \\ &= (\cos\theta) \left[\frac{\gamma_1}{\pi} \right]^{1/2} + (\sin\theta) W_{0\omega}. \end{aligned} \quad (4.8)$$

The secular equation $p(\omega)$ which defines the poles (resonances) of $a_i(\omega)$ is given by

$$\begin{aligned} p(\omega) &= [\delta(\omega) - \omega_{d_0} + i\tilde{\gamma}_0][\delta(\omega) - \omega_{d_1} + i\tilde{\gamma}_1] + \tilde{\gamma}_0\tilde{\gamma}_1 \\ &= [\delta(\omega) - \Gamma_0][\delta(\omega) - \Gamma_1]. \end{aligned} \quad (4.9)$$

Expressions (4.6)–(4.9) give the DRR basis explicitly (neglecting all shifts in keeping with the assumed coupling constants) from which the factors in the equation of motion (3.15) are easily constructed.

To demonstrate how the DRR works consider the photoelectron spectrum and the initial state population. Using definition (3.22) of the photoelectron spectrum $S(\omega)$ the result in the semiclassical limit is

$$\begin{aligned} S(\omega_0) &= \lim_{t \rightarrow \infty} \text{tr} [\hat{R}(t) \hat{\rho}_0 \hat{R}^\dagger(t) | \omega_0 \rangle \langle \omega_0 |] \\ &= \lim_{t \rightarrow \infty} \text{tr} [e^{-i\hat{h}_{\text{SC}} t} | 0 \rangle \langle 0 | e^{+i\hat{h}_{\text{SC}} t} | \omega_0 \rangle \langle \omega_0 |] \\ &= \lim_{t \rightarrow \infty} | J_{\omega_0}(t) |^2, \end{aligned} \quad (4.10)$$

where

$$\begin{aligned} J_{\omega_0}(t) &= \int d\omega e^{-i\delta(\omega)t} \langle \tilde{\omega} | 0 \rangle \langle \omega_0 | \tilde{\omega} \rangle \\ &= e^{-i\delta(\omega_0)t} \langle \tilde{\omega}_0 | 0 \rangle + r_{\omega_0}(t). \end{aligned} \quad (4.11)$$

In (4.10), $\hat{R}(t)$ is the evolution operator pertaining to the Hamiltonian \hat{h}_{SC} . In deriving (4.11) we used the expression for $\hat{R}(t)$ [Eq. (B4)], the fact that $[\hat{R}(t), |\omega_0\rangle\langle \omega_0|] = 0$ and the expression for $\langle \omega_0 | \tilde{\omega} \rangle$ from (4.7). As can be easily shown $\lim_{t \rightarrow \infty} r_{\omega_0}(t) = 0$ due to factors $e^{-\Gamma_i t}$ whenever both roots of the secular equation (4.9) have a nonvanishing imaginary part. This is the ‘‘nontrapping’’ case (see below). The same also holds true when either root of (4.9) is real (the ‘‘trapping’’ case) due to a vanishing multiplicative factor. Therefore

$$\begin{aligned} S(\omega_0) &= | \langle \tilde{\omega}_0 | 0 \rangle |^2, \\ \langle 0 | \tilde{\omega}_0 \rangle &= \frac{W_{0\omega} [\delta(\omega_0) - \Delta + \gamma_1 q]}{p(\omega_0)}, \end{aligned} \quad (4.12)$$

and for $|q| \rightarrow \infty$ (or $W_{0\omega} \rightarrow 0$) the numerator in (4.12) is to be replaced by $W_{01}(\gamma_1/\pi)^{1/2}$.

The simplicity of $S(\omega_0)$ is gratifying. The numerator exposes the Fano zero, as it should. The denominator im-

plies the interpretation of the two complex roots of the secular equation (4.9) as the location *and* width of the dressed resonances. The widths of the unperturbed dressed resonances, due to the static $V_{1\omega}$ mixing, can be identified with $\tilde{\gamma}_j$ [see Eq. (4.8)] and their energies with $\hbar\omega_{d_j}$.

As a second application consider the initial state population $P_0(t)$, defined in (3.21). The same steps in (4.10) yield⁵

$$P_0(t) = |J_0(t)|^2 \quad (4.13)$$

with

$$J_0(t) = \int d\omega e^{-i\delta(\omega)t} |\langle \bar{\omega} | 0 \rangle|^2 = \sum_j A_j e^{-i\Gamma_j t}, \quad (4.14)$$

where we used $[\hat{R}(t), |0\rangle\langle 0|] = 0$.

The simple result [(4.13) and (4.14)] offers a clear analysis of Rabi oscillations in the context of bound-continuum transitions: The oscillation frequency of $P_0(t)$, defined as the Rabi frequency Ω_R , is

$$\Omega_R(\Omega_0, q) = |\operatorname{Re}(\Gamma_0 - \Gamma_1^*)|. \quad (4.15)$$

By the same token, the long time limit of the $P_0(t)$ slope envelope is

$$s = \frac{1}{2} \min[|\operatorname{Im}(\Gamma_1 - \Gamma_j^*)|, i, j = 0, 1]. \quad (4.16)$$

Consequently we can define the “strong” and “weak” field regimes in the present context as corresponding to $\Omega_R \gg s$ or $\Omega_R \ll s$, respectively. A simplified definition of these two regimes is given in Sec. VI.

A corollary of (4.15) is the condition for population trapping.^{2,6,7,9} As a result of destructive interference between the $|0\rangle - |1\rangle$ and $|0\rangle - |\omega\rangle$ transitions some fraction of the population can remain trapped in the initial state so that $\lim_{t \rightarrow \infty} P_0(t) \neq 0$. For this to happen s must vanish; i.e., either Γ_0 or Γ_1 or both are purely real. The secular equation (4.9) implies that this occurs whenever

$$\tilde{\gamma}_0 \tilde{\gamma}_1 = 0. \quad (4.17)$$

Condition (4.17) simply states that for population trapping to occur, at least one of the dressed states has a vanishing width. This is a very plausible physical condition. By inserting in (4.17) expressions (4.8) and (3.25) we find the following parameter relation for trapping to occur:²

$$\left(\frac{\Omega_0}{\gamma_1} \right)_{\text{trapping}} = 4(1+q^2)(1-\Delta/\gamma_1 q). \quad (4.18)$$

For more complicated configurations, e.g., for several autoionizing states,¹⁰ the same physical argument leads to a trapping condition that equates the product of all the dressed-state widths to zero.

V. THE FULL PROBLEM: TWO ANALYTIC RESULTS PERTAINING TO RECYCLING AND PHASE-JITTER RELAXATION

The simplicity of the solution to the equations of motion in the semiclassical limit is lost when relaxations

are added. While the exact numerical solution of (3.13), in the general case, is deferred to Sec. VI and Appendixes C and D, we discuss here two analytic results pertaining to relaxations in specialized limits. Beyond these results, the equations must be solved numerically.

A. The photoelectron spectrum in the presence of recycling with no phase jitter

Consider the $\gamma_T = 0$ limit of the model and only the photoelectron spectrum $S(\omega)$.²² This quantity is expected to be simpler than $P_0(t)$ since it is observable in the $t \rightarrow \infty$ limit. The derivation, given in Appendixes D and E hinges on the argument that the form of $S(\omega)$ is known: As in the semiclassical limit given in Eq. (4.12), the numerator of $S(\omega)$ *must* reflect the Fano zero. This is because there cannot be decay from that particular energy level which is inaccessible for excitation due to complete destructive interference. By the same token, the denominator in $S(\omega)$ is expected to have *two* poles for the two dressed resonances in the model.

The existence of the new recycling decay channel modifies the width and location of the dressed resonances. In particular, as the recycling frequency γ_S [Eq. (3.26)] increases, the elastic and inelastic dressed resonances narrows and broadens, respectively. The physical origin of this behavior and examples are given in Sec. VI. Here we quote only the result (Appendix E),

$$S(\omega) = N \frac{|p(\omega)\langle 0 | \bar{\omega} \rangle|^2}{P(\omega, z=0)}, \quad (5.1)$$

where the modified secular equation function $P(\omega, z)$ is given by

$$1 + iQ(\omega_1) \int d\omega' \frac{|F(\omega')|^2}{iz + \delta(\omega_0) - \omega} = \frac{P(\delta(\omega_0), z)}{p(iz + \delta(\omega_0))}, \quad (5.2)$$

and $p(\omega_0)$ is the semiclassical secular function given by (4.9). The modified secular function $P(\delta(\omega_0), z)$ is quite complicated. However, by virtue of (3.25) and (3.17) an approximate form in the $|q| \ll 1$ and $|q| \gg 1$ limits, respectively, is obtained by inserting in (5.2)

$$|F(\omega)|^2 \cong \begin{cases} |F_B(\omega)|^2 + 2 \operatorname{Re}[F_B(\omega)F_C^*(\omega)] & \text{for } |q| \gg 1 \\ |F_C(\omega)|^2 + 2 \operatorname{Re}[F_C(\omega)F_B^*(\omega)] & \text{for } |q| \ll 1. \end{cases} \quad (5.3)$$

The physical content of the $|q| \gg 1$ and $|q| \ll 1$ limits is discussed in Sec. VI.

B. The substitution rule in the presence of phase-jitter relaxation

A quick proof of the substitution rule⁵ for including the γ_T -term effects into a $\gamma_T = 0$ calculation follows from (3.11). This equation implies that in the unperturbed representation or the SDR, the γ_T term contributes only for

$\hat{O}_A = |0\rangle\langle j|$, or its adjoint, since

$$[[|0\rangle\langle j|, |0\rangle\langle 0|], |0\rangle\langle 0|] = |0\rangle\langle j|. \quad (5.4)$$

For these \hat{O}_A only the first term on the RHS of (3.11) contributes

$$[|0\rangle\langle j|, \hat{h}_{SC}] = -i\Delta_j |0\rangle\langle j| + \dots, \quad (5.5)$$

where $\Delta_j = \omega_j - \omega_L$. This simple observation is the content of the substitution rule: By replacing

$$\begin{aligned} \pm i\Delta_j &\rightarrow \pm i\Delta_j - \gamma_T, \quad (\text{in } t \text{ domain}) \\ \pm i\Delta_j &\rightarrow \pm i\Delta_j + \gamma_T, \quad (\text{in } z \text{ domain}) \end{aligned} \quad (5.6)$$

in the equations of motion, the phase-jitter effects are included for *one-time* atomic observables expectation values. The “z domain” in (5.6) refers to the Laplace-transformed equations of motion (Appendix D). In the presence of recycling, the rule (5.6) obviously does not apply to the Δ_j factors in the recycling term of (3.15).

VI. THE FULL PROBLEM: NUMERICAL RESULTS AND DISCUSSION

Given the lack of analytical solutions to the full problem including relaxations, we base our discussion on a numerical solution of the model. The model can be solved exactly.³⁻⁵ We can therefore analyze systematically the solution in the various qualitatively different regimes of the physical-parameter space. Some segments of this parameter space have been discussed previously. For the sake of a unified point of view and completeness we examine here the whole parameter space.

The model depends on six parameters,

$$\Omega_0, q, \gamma_1, \Delta (= \omega_1 - \omega_L), \gamma_S, \gamma_T, \quad (6.1)$$

or

$$W_{01}, W_{0\omega}, \gamma_1, \Delta (= \omega_1 - \omega_L), \gamma_S, \gamma_T,$$

and the calculated quantities are the initial state population $P_0(t)$ and the photoelectron spectrum $S(\omega)$. The first four parameters in (6.1) specify the stimulated transitions. In previous literature the $\{\Omega_0, q, \gamma_1\}$ set is used, while this work implies that the equivalent $\{W_{01}, W_{0\omega}, \gamma_1\}$ set is more natural. The last two parameters, i.e., γ_S and γ_T , specify the relaxation processes. We first discuss the $\gamma_S = \gamma_T = 0$ subspace and then examine the effects of superimposing the relaxation processes.

The key observation is that the $\gamma_S = \gamma_T = 0$ subspace comprises two physically different regimes specified by $|q| \gg 1$ and $|q| \ll 1$, respectively (see Fig. 3). To demonstrate the point consider the limits $|q| = \infty$ and $q = 0$ separately. When $|q| = \infty$ it follows from (3.25) that $W_{01} \gg W_{0\omega}$, i.e., the continuum is populated *indirectly* via the autoionizing state $|1\rangle$ [see Fig. 1(a)]. Since the lifetime of $|1\rangle$ is γ_1 , the population rate of the continuum cannot exceed γ_1 , irrespective of the pump-laser strength parameter W_{01} . Consequently, two situations can arise: When $W_{01} \gg \gamma_1$ (and $W_{01} \gg \Delta$), i.e.,

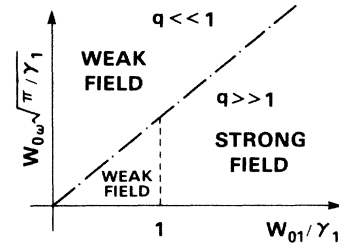


FIG. 3. Qualitatively different regimes in the unperturbed representation physical parameters space, see text. The chosen variables are all dimensionless.

when the Rabi oscillation frequency is larger than the decay rate of the upper level to the continuum, then $P_0(t)$ exhibits oscillatory behavior, i.e., Rabi oscillations. This is therefore a “strong-field” regime. On the other hand, when $W_{01} \ll \gamma_1$, the population of the $|1\rangle$ state decays faster than the Rabi frequency W_{01} . Hence the Rabi oscillations are quenched and $P_0(t)$ exhibits an exponentially decaying behavior which is a “weak field” characteristic (Fig. 3).

When $q = 0$ the situation is quite different. Now $W_{01} \ll W_{0\omega}$ [Eq. (3.25)], i.e., the continuum is populated *directly* from the initial state $|0\rangle$. However, since the continuum is flat, electron probability transferred to the continuum never comes back. Therefore for $|q| \ll 1$ the initial state population $P_0(t)$ experiences only decay, i.e., $|q| \ll 1$ is always a weak-field regime (Fig. 3). This weak-field regime, however, is different in nature from its counterpart when $|q| \gg 1$. Since the continuum is populated directly, the ever stronger the laser intensity is, the ever faster the $|0\rangle$ level is depleted. This is to be contrasted with the situation for $|q| \gg 1$, in which the initial state depletion rate cannot exceed γ_1 irrespective of the driving-laser strength.

These remarks are borne out in the following widths

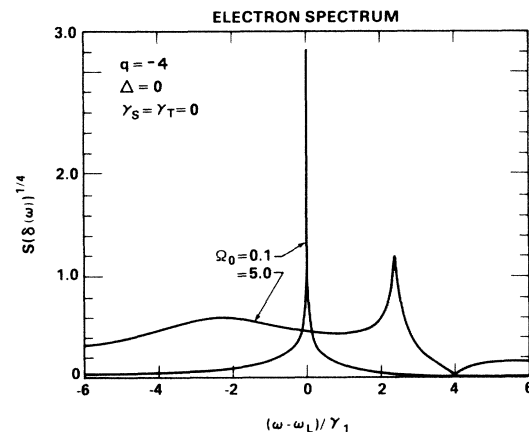


FIG. 4. Photo-electron spectrum for a $|q| \gg 1$ case with no relaxations in the weak- and strong-field regimes. The SDR parameters in units of γ_1 are indicated. The Fano zero ω_F is at $\omega_F = \Delta - \gamma_1 q = 4\gamma_1$. The narrowed asymmetric line shape is evident in the strong-field case.

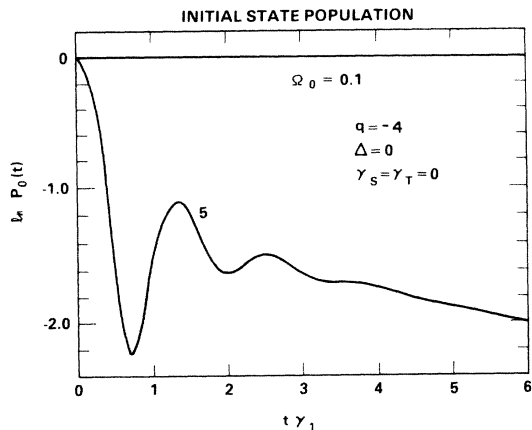


FIG. 5. The log plot of the initial state population corresponding to Fig. 4. The SDR parameters in units of γ_1 are indicated. The strong-field case $\Omega_0=5$ shows attenuated Rabi oscillations, while for the weak-field case the initial state population is depleted exponentially.

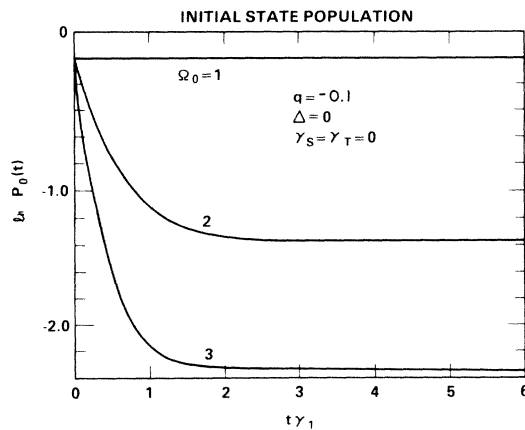


FIG. 7. The log plot of the initial state population for a $q \ll 1$ case. The SDR parameters in units of γ_1 are indicated. The two-slope characteristic in the strong-field case is evident.

sum rule:

$$\begin{aligned} \Gamma_1 + \Gamma_2 &= \tilde{\gamma}_0 + \tilde{\gamma}_1 = \gamma_1 + \pi |W_{0\omega}|^2 \\ &\cong \gamma_1 \text{ for } q \gg 1 \\ &\cong \pi |W_{0\omega}|^2 \text{ for } q \ll 1, \end{aligned} \quad (6.2)$$

where (4.8) was used. In the $q \gg 1$ regime we distinguish between two domains (Fig. 3). In the weak-field domain i.e., $W_{01} \ll \gamma_1, \Delta$ it follows that $\tilde{\gamma}_1 \sim \gamma_1 \gg \tilde{\gamma}_0$. Therefore, as discussed above, Rabi oscillations do not occur. On the other hand, in the strong-field domain $W_{01} \gg \gamma_1, \Delta$, i.e., $\tilde{\gamma}_0 \sim \tilde{\gamma}_1 \sim \gamma_1/2$. In this domain Rabi oscillations between the two dressed resonances do occur. They are damped, however, since the electron has a finite probability to escape to the continuum in each $|0\rangle - |1\rangle$ lap. The $q \ll 1$ regime is qualitatively different. Equations (3.25), (4.4),

and (6.2) imply that $W_{0\omega} \sim \tilde{\gamma}_0 \gg \tilde{\gamma}_1$, i.e., the elastic dressed resonance decays directly.

These features of the dressed states are reflected in the behavior of $S(\omega)$ and $P_0(t)$ [see Eqs. (4.12) and (4.13)]. Figures 4 and 5 show results in the $|q| \gg 1$ regime in the strong- and weak-field limits. The weak-field example is characterized by a very narrow elastic peak at $\delta(\omega) = \omega - \omega_L \approx 0$, of width given by (4.8), or better yet, by the solution of the secular equation (4.9). The broad inelastic electron peak with width $\tilde{\gamma}_1$ is not seen since it is barely populated. The strong-field example shows the two dressed resonances. The peak near the Fano zero is narrowed and distorted,^{1,2} reflecting the effect of destructive interference of the two pathways which populate the continuum. The corresponding $P_0(t)$ is given in Fig. 5. The strong-field case shows damped Rabi oscillations, while the weak field exhibits an exponential decay.

Figures 6 and 7 are examples of the $|q| \ll 1$ regime.

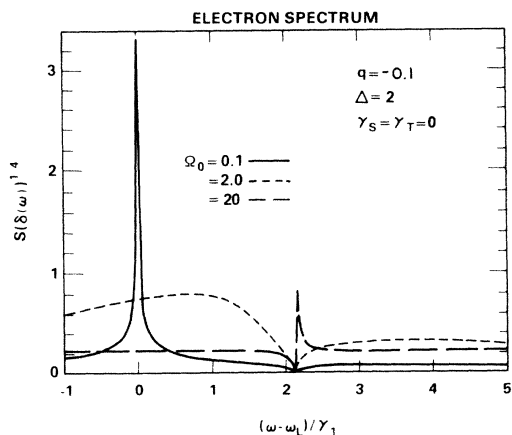


FIG. 6. The photoelectron spectrum for a $|q| \ll 1$ case with no relaxations in the weak- and strong-field regimes. The SDR parameters in units of γ_1 are indicated. The weak-field curve shows only the elastic peak. The inelastic peak around $\delta(\omega) \sim 2$ is too narrow to be resolved. Increasing Ω_0 broadens and shifts the elastic and inelastic peaks to the point when the latter is resolved and the former disappears.

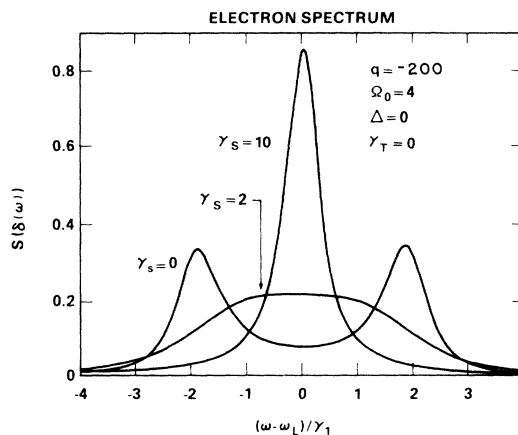


FIG. 8. Photoelectron spectrum for a $|q| \gg 1$ case in the presence of recycling but no phase-jitter relaxations. The SDR parameters and recycling rate γ_S , in units of γ_1 , are indicated. Note the transition from an Autler-Townes double peak for $\gamma_S = 0$ to an ever-narrower elastic peak at $\delta(\omega) = 0$.

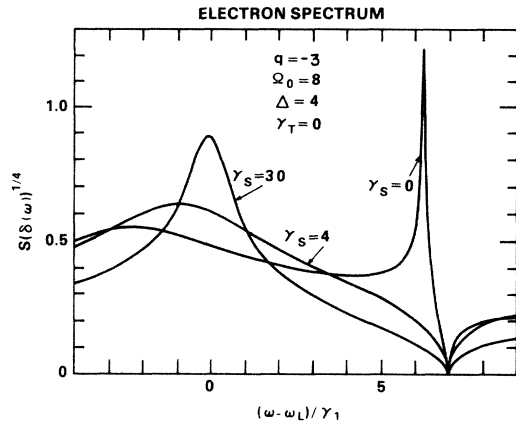


FIG. 9. The photoelectron spectrum for a $|q| > 1$ case in the presence of recycling, with no phase-jitter relaxation. The SDR parameters and γ_S in units of γ_1 are indicated. The Fano zero is at $\delta(\omega) = 7$. Note that as γ_S increases, the asymmetric inelastic peak around $\delta(\omega) = 6$ is broadened, and the emergence of the ever-narrowed elastic peak around $\delta(\omega) = 0$ is seen.

In this case Eqs. (4.8) and (6.2) imply that the elastic peak in $S(\omega)$ is ever broadened as the laser strength increases. The inelastic peak at $\delta(\omega) \sim |\Delta|$ is, on the contrary, very narrow to the point of not being resolved in the figures for the small Ω_0 case. A corresponding $P_0(t)$ behavior (Fig. 7) shows an interesting two-slope structure: The first slope, which controls the short-time behavior, increases with the driving-laser strength, while the second, almost vanishing slope at longer times hardly depends on the driving-laser strength. In terms of our physical picture, the first slope is associated with the direct depletion of $|0\rangle$, while the second slope represents a slow depletion of $|0\rangle$ via the autoionizing state $|1\rangle$.

We turn now to discuss the effect of the relaxations. The qualitative effect of radiative recycling is the follow-

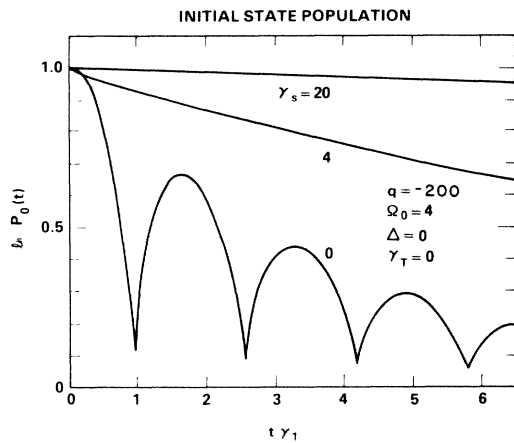


FIG. 10. The log plot of the initial state population corresponding to Fig. 8. The SDR parameters and γ_S in units of γ_1 are indicated. Starting from the attenuated Rabi oscillations for $\gamma_S = 0$ the curve becomes linear for large γ_S , is characteristic of a weak-field domain.

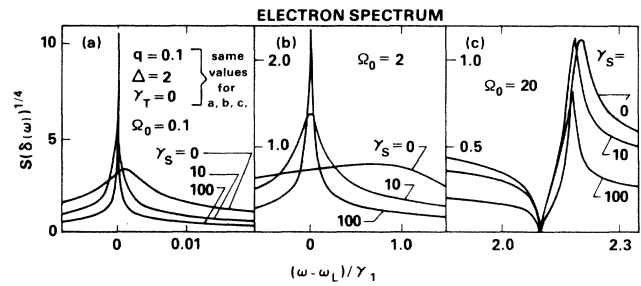


FIG. 11. Effect of recycling on the photoelectron spectrum corresponding to the $|q| \ll 1$ case of Fig. 6. (a), (b), (c) probe three adjacent sections of the spectrum. The narrowing (broadening) effect of recycling on the elastic (inelastic) peaks, respectively, is evident.

ing. As the recycling frequency γ_S increases, the fraction of time the atom spends in the initial state increases since recycling arises from *decay back* to the initial state. Consequently an increase in γ_S suppresses the oscillations in $P_0(t)$, narrows the elastic peak, and broadens the inelastic peak in $S(\omega)$.^{4,5} These features occur irrespective of the stimulated transitions' parameters. The examples in Figs. 8–12 demonstrate these remarks.

Figure 8 is a particularly simple case where for $\gamma_S = 0$ the spectrum $S(\omega)$ shows an Autler-Townes double-hump line shape.^{2,23} This is therefore a strong-field, $|q| \gg 1$ case. When $2\gamma_S = \Omega_0 = 4$, i.e., when the recycling frequency is equal to the Rabi frequency, there is a transition to the single, ever narrower elastic peak at $\Delta = 0$ characteristic of a *weak-field* situation. A more typical $|q| \gg 1$ example of elastic peak narrowing is given in Fig. 9: The $\delta(\omega) \approx 0$ peak is ever narrowed as γ_S increases, while the narrow inelastic peak around $\delta(\omega) \approx \Delta$ is broadened and eliminated. The corresponding behavior of $P_0(t)$, shown

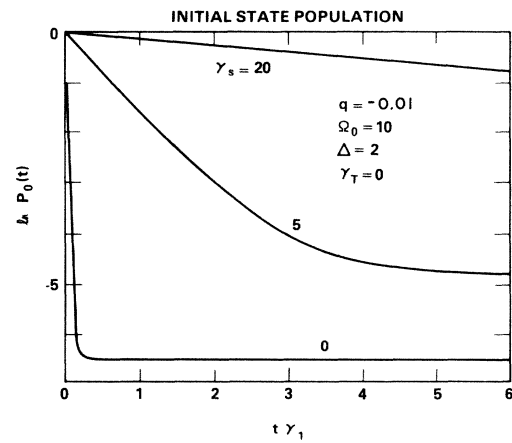


FIG. 12. Log plot of the initial state population for a $|q| \ll 1$ case in the presence of recycling. The SDR parameters and γ_S in units of γ_1 are indicated. Note the dramatic change from a two-slope structure for $\gamma_S = 0$ to a linear dependence as γ_S increases.

in Fig. 10, demonstrates the suppression of the Rabi oscillations.

Figures 11 and 12 are examples for the $|q| \ll 1$ domain. Figure 11, with the parameters of Fig. 6, shows the γ_S effects on the elastic and inelastic peaks. The former is narrowed, and the latter is broadened irrespective of $W_{0\omega}$. The dramatic effect on $P_0(t)$ is shown in Fig. 12: Increase in γ_S suppresses the two-slope behavior, yielding a single ever-decreasing slope which indicates a long lifetime of $|0\rangle$.

The effect of the phase-jitter relaxation has been discussed elsewhere.³⁻⁵ This relaxation mechanism endows the driving laser with an effective band width γ_T . Consequently, the two dressed resonances in $S(\omega)$ are broadened and correspondingly $P_0(t)$ is depleted faster. It follows, therefore, that there is a competition between the γ_T and γ_S relaxations with regard to the elastic peak, i.e., narrowing versus broadening, while both act in concert to broaden the inelastic peak. This competition has been demonstrated elsewhere.⁴

In summary, the qualitative features of the observables discussed, e.g., the photoelectron spectrum, reflect the existence of the two underlying dressed resonances which originate from the initial and autoionizing states. The locations and widths of the resonance are determined by the interplay between the stimulated and relaxation-assisted transitions. The DRR is the natural representation for this class of systems since it incorporates the stimulated transitions from the outset and the corresponding expressions are simple. The systematic analysis of the exact results provides a clear understanding of the effects due to laser stimulation and to the recycling and phase-jitter relaxation mechanisms. We hope the DRR may prove useful in other applications, e.g., to simplify the calculation of light scattering by an autoionizing state.^{3,18}

$$\int d\omega_\lambda \omega_\lambda \int d\omega d\omega' \Omega_\lambda^*(\omega) \Omega_\lambda(\omega') \int_0^t d\tau e^{-i(\omega_\lambda - i\eta)(t-\tau)} ([\hat{O}_A(t), \hat{B}^\dagger(\omega)])_H(t) (\hat{B}(\omega'))_H(\tau). \quad (\text{A4})$$

Now since $\Omega_\lambda(\omega)$ [Eq. (2.6)] and the radiation-modes spectrum are infinitely broad, the ω_λ integration implies $|t-\tau| \sim \tau_c \sim 10^{-18}$ sec, where τ_c is a cutoff set as the transit time for light across an atom. Next, define¹⁶ an envelope dipole operator \hat{B}_S by $[\hat{B}(\omega)]_H(t) = e^{i\omega t} \hat{B}_S(\omega, t)$, where $\hat{B}_S(\omega, t)$ is expected to vary over typical slow atomic time scales τ_A such as the Rabi frequency. Consequently, as long as $\tau_A \gg \tau_c$, it is allowed to approximate $\hat{B}_S(\omega, \tau) \approx \hat{B}_S(\omega, t)$ under the integral sign and the Markov approximation follows.

For typical discrete transitions in the optical-frequency domain this condition is well satisfied. For continuum transitions, however, the very high and very low transition frequencies pose a problem. When ω is very high, such that $\langle \omega \rangle \sim \tau_c^{-1}$, the Markov approximation obviously breaks down. For very low frequencies ω , the rotating-wave approximation¹⁴ underlying (2.4) may become invalid. Thus the basic premises of (3.1) are valid only within a frequencies band. When $q \gg 1$, the Fano profile

ACKNOWLEDGMENTS

We wish to thank Mr. Z. Deng and Dr. E. Kyrölä for stimulating discussions, and Professor D. S. Koltun for an enlightening exchange. This work has been supported by the U. S. Air Force Office of Scientific Research under Contract No. AFOSR-81-0204-A.

APPENDIX A: THE MARKOV-BORN APPROXIMATION

This approximation^{16,17} underlies the elimination of the radiation-field operators from the equations of motion for the atomic operator $\hat{O}_A(t)$. The argument for such an elimination, in the context of continuum transitions, is demonstrated by considering a typical term in the equation of motion for $\hat{O}_A(t)$ in the unperturbed representation,

$$[\hat{O}_A, \hat{H}_{\text{INT}}] \alpha \sum_\lambda \int d\omega \mathfrak{K} \Omega_\lambda^*(\omega) ([\hat{O}_A(t), \hat{B}^\dagger(\omega)])_H \hat{a}_\lambda(t) \quad (\text{A1})$$

and

$$\hat{a}_\lambda(t) = \hat{a}_\lambda^{(v)}(t) - i \int_0^t d\tau G_\lambda^R(t-\tau) \int d\omega \Omega_\lambda(\omega) (\hat{B}(\omega))_H(\tau) \quad (\text{A2})$$

with¹⁴

$$\hat{a}_\lambda^{(v)}(t) = \hat{a}_\lambda e^{-i\omega_\lambda t}$$

and

$$G_\lambda^R(t-\tau) = e^{-i(\omega_\lambda - i\eta)(t-\tau)}.$$

By inserting (A2) into (A1) and replacing the λ summation by an integration one finds the RHS proportional to

naturally defines a frequency band around the autoionizing state. When $q \ll 1$, however, the relevant transition frequency band must be delineated in some other way. In our approach this is implicitly done in (3.18) by invoking $Q(\omega) = Q(\omega_1)$. With these provisos it is permissible in (A4) to replace $B_S(\omega, \tau)$ by $B_S(\omega, t)$ so that

$$(\hat{B}(\omega))_H(\tau) = e^{-i\omega(\tau-t)} (\hat{B}(\omega))_H(t). \quad (\text{A5})$$

This is one form of the Markov approximation, which leads to (3.1).

APPENDIX B: TRANSFORMATION TO THE ROTATING FRAME AND THE DRR

The rotating frame is defined as the frame in which $\hat{H}_{\text{SC}}^{(0)}(t)$, given in Eq. (3.5), is time independent. Hence, if we define

$$\hat{H}_{\text{SC}}^{(0)} = \hat{R}_0(t) \hat{h}_{\text{SC}}^{(0)} \hat{R}_0^\dagger(t),$$

then simple algebra yields

$$\hat{R}_0(t) = |0\rangle\langle 0| + e^{-i\omega_L t} [|1\rangle\langle 1| + \int d\omega |\omega\rangle\langle \omega|]. \quad (\text{B1})$$

Note that $\hat{R}_0(t)$ is determined only up to a phase. Correspondingly the Schrödinger equation $i\hbar d/dt |\psi(t)\rangle = \hat{H}_{\text{SC}}^{(0)} |\psi(t)\rangle$ is transformed into

$$i \frac{d}{dt} |\phi(t)\rangle = \hat{h}_{\text{SC}} |\phi(t)\rangle, \quad (\text{B2})$$

where

$$\begin{aligned} |\phi(t)\rangle &= \hat{R}_0^\dagger(t) |\psi(t)\rangle, \\ \hat{h}_{\text{SC}} &= \hat{h}_{\text{SC}}^{(0)} - i \hat{R}_0^\dagger(t) \frac{d}{dt} \hat{R}_0(t) \end{aligned} \quad (\text{B3})$$

and \hat{h}_{SC} is given by (3.9). From (B2) and (B3) it follows that the evolution operator $\hat{R}(t)$ and density matrix $\hat{\rho}(t)$ pertaining to $\hat{H}_{\text{SC}}^{(0)}(t)$ are

$$\begin{aligned} \hat{R}(t) &= \hat{R}_0(t) \exp(-i\hat{h}_{\text{SC}} t), \\ \hat{\rho}(t) &= \hat{R}(t) \hat{\rho}_0 \hat{R}^\dagger(t). \end{aligned} \quad (\text{B4})$$

APPENDIX C: THE EQUATIONS OF MOTION IN THE SDR REPRESENTATION

A considerable body of literature¹⁻⁹ as well as the exact numerical solution of the model were carried out in the SDR representation [see Sec. I and Fig. 1(b)]. The basis states of the SDR is comprised of the initial state $|0\rangle$ and the perturbed continuum states $|\omega_{\text{SD}}\rangle$ resulting from the admixture of the autoionizing state $|1\rangle$ and the unperturbed continuum states $|\omega\rangle$. The Fano profile $F_0(\omega)$ [Eq. (3.23)] is, correspondingly, the dipole matrix element between $|0\rangle$ and $|\omega_{\text{SD}}\rangle$,

$$F_0(\omega) \sim W_{01} \langle 1 | \omega_{\text{SD}} \rangle + W_{0\omega} \langle \omega | \omega_{\text{SD}} \rangle. \quad (\text{C1})$$

Since in the SDR the states $|0\rangle$ and $|1\rangle$ are *not* treated on an equal footing, a complete set of atomic projection operators are²

$$\begin{aligned} \hat{P}_0 &= |0\rangle\langle 0|, \quad \hat{C}_{\text{SD}}(\omega, \omega') = |\omega_{\text{SD}}\rangle\langle \omega'_{\text{SD}}|, \\ \hat{B}_{\text{SD}}(\omega) &= |0\rangle\langle \omega_{\text{SD}}|, \quad \hat{B}_{\text{SD}}^\dagger(\omega) = |\omega_{\text{SD}}\rangle\langle 0|. \end{aligned} \quad (\text{C2})$$

Straightforward algebra, with use of the Markov-Born approximation, gives the equations of motion for the expectation values,

$$O(t) = \langle \text{tr} \hat{\rho}(t) \hat{O} \rangle, \quad (\text{C3})$$

where $\hat{\rho}(t)$ is the total density matrix, $\langle \rangle$ indicates an ensemble average, and tr is a trace over the atomic and radiative degrees of freedom. The equations of motion are⁴⁻⁵

$$\begin{aligned} \frac{d}{dt} P_0(t) &= - \int d\omega [F_0^*(\omega) B_{\text{SD}}^*(\omega; t) + F_0(\omega) B_{\text{SD}}(\omega; t)] + \int d\omega d\omega' [F_0^*(\omega) R_{\text{SD}}(\omega') + F_0(\omega') R_{\text{SD}}^*(\omega)] C_{\text{SD}}(\omega, \omega'; t), \\ \frac{d}{dt} B_{\text{SD}}(\omega_0; t) &= [-i(\omega_0 - \omega_L) - \gamma_T] B_{\text{SD}}(\omega_0; t) + F_0^*(\omega_0) P_0(t) \\ &\quad - \int d\omega' F_0^*(\omega') C_{\text{SD}}(\omega', \omega_0; t) - F_0^*(\omega_0) \int d\omega' R_{\text{SD}}(\omega') B_{\text{SD}}(\omega'; t), \\ \frac{d}{dt} C_{\text{SD}}(\omega_0, \omega'_0; t) &= i(\omega_0 - \omega'_0) C_{\text{SD}}(\omega_0, \omega'_0; t) + F_0^*(\omega'_0) B_{\text{SD}}^*(\omega_0; t) + F_0(\omega_0) B_{\text{SD}}(\omega'_0; t) \\ &\quad - \int d\omega' [F_0^*(\omega'_0) R_{\text{SD}}(\omega') C_{\text{SD}}(\omega_0, \omega'; t) + F_0(\omega_0) R_{\text{SD}}^*(\omega') C_{\text{SD}}(\omega', \omega'_0; t)], \end{aligned} \quad (\text{C4})$$

and $R_{\text{SD}}(\omega) = Q(\omega_1) F_0(\omega)$, where $Q(\omega_1)$ is given in (3.18). A comparison of (C4) with (3.15) underscores the simplification introduced by employing the DRR.

APPENDIX D: EXACT SOLUTION OF THE EQUATIONS OF MOTION

The equations of motion in the SDR, Eq. (C4), or in the DRR, Eq. (3.15), are linear, first order in time, and with time-independent coefficients. Hence the Laplace-transform method is particularly suitable. Define

$$F(z) = \int_0^\infty dt e^{-zt} F(t), \quad F(t) = \frac{1}{2\pi i} \int_C dz e^{zt} F(z), \quad (\text{D1})$$

where C is a contour parallel to the imaginary axis and located to the right of all singularities of $F(z)$ in the z plane. Then the corresponding equations for $P_0(z)$, $B_{\text{SD}}(\omega_0; z)$, and $C_{\text{SD}}(\omega_0, \omega'_0; z)$ or $C(\omega_0, \omega'_0; z)$ become algebraic. In the case of the SRD, the solution strategy is first to express $C_{\text{SD}}(\omega_0, \omega'_0; z)$ in terms of $B_{\text{SD}}(\omega_0; z)$ and $B_{\text{SD}}^*(\omega_0; z)$, to insert the result in the other two equations and solve for $B_{\text{SD}}(\omega_0; z)$ in terms of $P_0(z)$, and finally to solve the algebraic equation for $P_0(z)$. This straightforward yet tedious procedure works due to the simple Lorentzian form of $F_0(\omega)$, Eq. (3.23), which leads to a *separable* equation.⁴ We outline the corresponding steps in conjunction with the DRR. These results are then used in Appendix E.

In the absence of phase-jitter relaxation ($\gamma_T = 0$), the

Laplace-transformed equation of motion (3.15) takes the form

$$\begin{aligned} & [z - i(\omega_0 - \omega'_0)]C(\omega_0, \omega'_0; z) \\ &= [1 + M(z)] \langle 0 | \tilde{\omega}_0 \rangle \langle \tilde{\omega}'_0 | 0 \rangle \\ & \quad - \int d\omega' [F^*(\omega'_0)R(\omega')C(\omega_0, \omega'; z) \\ & \quad + F(\omega_0)R^*(\omega')C(\omega', \omega'_0; z)] , \end{aligned} \quad (D2)$$

where the initial conditions $C(\omega_0, \omega'_0; t=0)$ [see Eq. (3.20)] have been incorporated and $M(z)$ is the Laplace transform of $M(t)$. We now introduce the definitions

$$\begin{aligned} & [z - i(\omega_0 - \omega'_0)]C(\omega_0, \omega'_0; z) = D(\omega_0, \omega'_0; z) , \\ & A_0(\omega_0, \omega'_0; z) = \langle 0 | \tilde{\omega}_0 \rangle \langle \tilde{\omega}'_0 | 0 \rangle [1 + M(z)] , \\ & K_0(\omega_0, \omega'_0; z) = \frac{R(\omega'_0)}{z - i(\omega_0 - \omega'_0)} , \end{aligned} \quad (D3)$$

$$f(\omega_0, z) = \int d\omega'_0 K_0(\omega_0, \omega'_0; z) D(\omega_0, \omega'_0; z) .$$

In terms of (D3), the equation of motion (D2) takes the canonical form,

$$\begin{aligned} D(\omega_0, \omega'_0; z) &= A_0(\omega_0, \omega'_0; z) - F^*(\omega'_0) f(\omega_0; z) \\ & \quad - F(\omega_0) f^*(\omega'_0; z) . \end{aligned} \quad (D4)$$

Equation (D4) can be "solved" for $D(\omega_0, \omega'_0; z)$ since it has a separable structure: Applying $\int d\omega'_0 K_0(\omega_0, \omega'_0; z)$ to (D4) gives, after some manipulations,

$$f(\omega_0, z) = A_3(\omega_0, z) + \int d\omega''_0 K_1(\omega_0, \omega''_0; z) f(\omega''_0, z) , \quad (D5)$$

where

$$\begin{aligned} A_3(\omega_0, z) &= A_2(\omega_0, z) \\ & \quad - B_2(\omega_0, z) \int d\omega'_0 K_0(\omega_0, \omega'_0; z) A_2^*(\omega'_0; z) , \\ K_1(\omega_0, \omega''_0; z) &= B_2(\omega_0, z) \int d\omega'_0 K_0(\omega_0, \omega'_0; z) B_2^*(\omega'_0; z) \\ & \quad \times K_0^*(\omega'_0, \omega''_0; z) , \\ A_2(\omega_0, z) &= \frac{A_1(\omega_0, z)}{1 + B_1(\omega_0, z)} , \\ B_2(\omega_0, z) &= \frac{F(\omega_0)}{1 + B_1(\omega_0, z)} , \\ A_1(\omega_0, z) &= \int d\omega'_0 K_0(\omega_0, \omega'_0; z) A_0(\omega_0, \omega'_0; z) , \\ B_1(\omega_0, z) &= \int d\omega'_0 K_0(\omega_0, \omega'_0; z) F^*(\omega'_0) . \end{aligned} \quad (D6)$$

Provided the kernel $K_1(\omega_0, \omega''_0; z)$ in (D5) is separable, we can solve for $f(\omega_0, z)$. This is the case when $F(\omega)$ is comprised of one pole, as in the Fano profile $F_0(\omega)$, or a product of poles, as in the DRR. Finally, $M(z)$ is determined self-consistently.

The inversion (D1) to the time domain is done numerically, by converting the Laplace transform to a Fourier transform and evaluating the latter with the fast-Fourier-transform algorithm. To suppress ripples from edge effects

we added²⁴ to the inverted function a "cosine window," i.e., $f(i) = 0.5I(i)\{1 - \cos[2\pi(i-1)/N]\}$, where $I(i)$ are the unsmoothed values of the function and N (even) is the number of grid values and $1 \leq i \leq N+1$.

APPENDIX E: THE SECULAR EQUATION FOR THE PHOTOELECTRON SPECTRUM IN THE PRESENCE OF RECYCLING

We derive Eq. (5.1) by means of a combination of algebraic steps and an argument that hinges on the known structure of the expression of the photoelectron spectrum, namely, the presence of the Fano zero in the numerator (through a $\langle 0 | \tilde{\omega} \rangle$ factor) and two poles in the denominator. This form follows from the physical arguments discussed in the text. We therefore seek to identify such factors in the exact solution. The notation of Appendix D is used throughout. Only the infinite-time solution is needed, hence we set $z=0$.

Consider first the $q = \infty$ case. Equation (3.17) gives

$$\begin{aligned} F(\omega_0) &= W_{01} \langle 1 | \tilde{\omega}_0 \rangle , \\ \langle 1 | \tilde{\omega}_0 \rangle &= \left[\frac{\gamma_1}{\pi} \right]^{1/2} \frac{1}{p(\omega_0)} \\ & \quad \times \left[\delta(\omega_0) + W_{01} W_{0\omega} \left[\frac{\pi}{\gamma_1} \right]^{1/2} \right] , \end{aligned} \quad (E1)$$

and denote [see (D6)]

$$1 + B_1(\omega_0, z) = \frac{P(\omega_0, z)}{(iz + \omega_0 - \Gamma_0)(iz + \omega_0 - \Gamma_1)} , \quad (E2)$$

where $P(\omega_0, z)$ is a polynomial of second order in ω_0 . Lengthy algebra following Appendix D leads to the following forms:

$$\begin{aligned} f(\omega_0, z) &= \frac{P_4(\omega_0, z)}{D_6(\omega_0, z)} , \\ D(\omega_0, \omega'_0; z) &= \frac{P_{5,5}(\omega_0, \omega'_0; z)}{D_6(\omega_0, z) D_6^*(\omega'_0, z)} \\ D_6(\omega_0, z) &= p(\omega_0, z) (iz + \omega_0 - \Gamma_0) \\ & \quad \times (iz + \omega_0 - \Gamma_1) P(\omega_0, z) , \end{aligned} \quad (E3)$$

where $P_4, P_{5,5}$ are polynomials of orders 4 and 5 (in ω_0, ω'_0), respectively. The important point in (E3) is the denominator D_6 . Since *only* $P(\omega_0, z)$ depends on the recycling frequency γ_s , the other four factors in $D_6(\omega_0, z)$ must cancel factors in the numerator of $D(\omega_0, \omega'_0; z)$. Since the numerator is of order 5 in ω_0, ω'_0 , the cancellation leaves linear factors in ω_0, ω'_0 in the numerator which must express the Fano zero. Therefore

$$S(\omega_0) \alpha D(\omega_0, \omega_0; z=0) = N \frac{[\delta(\omega_0) - \Delta + \gamma_1 q]^2}{|P(\omega_0; z=0)|^2} . \quad (E4)$$

Consider now the $q=0$ limit when [recall Eq. (3.17)]

$$F(\omega_0) = W_{0\omega} \frac{[\delta(\omega_0) - \omega_{d_0}][\delta(\omega_0) - \omega_{d_1}]}{p(\omega_0)}. \quad (\text{E5})$$

Using the same steps as in the $q = \infty$ case we realize that

$D(\omega_0, \omega'_0; z)$ is again a rational function, with a denominator given by a product $D_6^*(\omega_0, z)D_6(\omega'_0, z)$, as in Eq. (E3). Hence the form (E4) must follow. Finally, since the $F(\omega)$ factor for a general q is a sum of (E5) and (E1), [Eq. (3.17)], the forms (E4) and (E2) are always valid.

- ¹P. Lambropoulos and P. Zoller, *Phys. Rev. A* **24**, 379 (1981); see also P. Lambropoulos, *Appl. Opt.* **19**, 3926 (1980).
- ²(a) K. Rzazewski and J. H. Eberly, *Phys. Rev. Lett.* **47**, 408 (1981); (b) K. Rzazewski and J. H. Eberly, *Phys. Rev. A* **27**, 2026 (1983).
- ³G. S. Agarwal, S. L. Haan, K. Burnett, and J. Cooper, *Phys. Rev. Lett.* **48**, 1164 (1982); S. L. Haan and G. S. Agarwal in *Proceedings of the Sixth International Conference on Spectral Lineshapes*, edited by K. Burnett (de Gruyter, Berlin, 1982), p. 1013; G. S. Agarwal, S. L. Haan, K. Burnett, and J. Cooper, *Phys. Rev. A* **26**, 2277 (1982); G. S. Agarwal, S. L. Haan, and J. Cooper, *ibid.* **28**, 1154 (1983); G. S. Agarwal, S. L. Haan, and J. Cooper, *ibid.* **29**, 2552 (1984); **29**, 2565 (1984); *Phys. Rev. Lett.* **52**, 1480 (1984).
- ⁴J. H. Eberly, K. Rzazewski, and D. Agassi, *Phys. Rev. Lett.* **49**, 693, (1982); G. S. Agarwal and D. Agassi, *Phys. Rev. A* **27**, 2254 (1983); D. Agassi, K. Rzazewski, and J. H. Eberly, *ibid.* **28**, 3648 (1983).
- ⁵D. Agassi in *Quantum Electrodynamics and Quantum Optics*, edited by A. O. Barut (Plenum, New York, 1984), pp. 167–194.
- ⁶M. Lewenstein, J. W. Haus, and K. Rzazewski, *Phys. Rev. Lett.* **50**, 417 (1983); J. W. Haus, M. Lewenstein, and K. Rzazewski, *Phys. Rev. A* **28**, 2269 (1983); J. W. Haus, K. Rzazewski, and J. H. Eberly, *Opt. Commun.* **46**, 191 (1983).
- ⁷P. E. Coleman and P. L. Knight, *Phys. Lett. A* **81**, 378 (1981); *J. Phys. B* **14**, 2138 (1981); *ibid.* **15**, L235 (1982); P. E. Coleman, P. L. Knight, and K. Burnett, *Opt. Commun.* **42**, 171 (1982); 1957(E) (1982); P. M. Radmore and P. L. Knight, *J. Phys. B* **15**, 561 (1982); B. J. Dalton and P. L. Knight, in *Proceedings of the Third New Zealand Symposium on Laser Physics*, edited by D. F. Walls (Springer-Verlag, Berlin, 1983).
- ⁸A. I. Andryushin, M. V. Fedorov, and A. E. Kazakov, *J. Phys. B* **15**, 2851 (1982); A. I. Andryushin, A. E. Kazakov and M. F. Fedorov, *Zh. Eksp. Teor. Fiz.* **82**, 91 (1982) [*Sov. Phys.—JETP* **55**, 53 (1982)]; A. I. Andryushin, M. V. Fedorov and A. E. Kazakov, *Opt. Commun.* **49**, 120 (1984).
- ⁹L. Armstrong, Jr., B. L. Beers, and S. Feneuille, *Phys. Rev. A* **12**, 1903 (1975); M. Crance and L. Armstrong, Jr., *J. Phys. B* **15**, 3199 (1982).
- ¹⁰Z. Deng, *Opt. Commun.* **48**, 284 (1983); Z. Deng and J. H. Eberly, *J. Opt. Soc. Am. B* **1**, 102 (1984).
- ¹¹C. Cohen-Tannoudji and S. Reynaud, in *Proceedings of the International Conference on Multiphoton Processes*, edited by J. H. Eberly and P. Lambropoulos (Wiley, New York, 1977); *J. Phys. B* **10**, 345 (1977).
- ¹²E. Courtens and A. Szoke, *Phys. Rev. A* **15**, 1588 (1977).
- ¹³U. Fano, *Phys. Rev.* **124**, 1866 (1961).
- ¹⁴See, for instance, L. Allen and J. H. Eberly, *Optical Resonance and Two-Level Atoms* (Wiley, New York, 1975), Chap. 7.
- ¹⁵See, for example, W. E. Cooke, T. F. Gallagher, S. A. Edelstein, and R. M. Hill, *Phys. Rev. Lett.* **40**, 178 (1978); S. Feneuille, S. Liberman, J. Pinard, and A. Taleb, *ibid.* **42**, 1404 (1979); T. S. Luk, L. DiMauro, T. Bergeman, and H. Metcalf, *ibid.* **47**, 83 (1981); E. Trefftz, *J. Phys. B* **16**, 1247 (1983).
- ¹⁶J. R. Ackerhalt and J. H. Eberly, *Phys. Rev. D* **10**, 3350 (1974); P. W. Milonni and W. A. Smith, *Phys. Rev. A* **11**, 814 (1975); P. W. Milonni, *Phys. Rep. C* **25**, 1 (1976); H. J. Kimble and L. Mandel, *Phys. Rev. A* **13**, 2123 (1976). See also G. S. Agarwal, Ref. 17.
- ¹⁷G. S. Agarwal, *Quantum Optics*, Vol. 7 of *Springer Tracts in Modern Physics*, (Springer, Berlin, 1974), Chap. 6.
- ¹⁸See, for instance, J. W. Haus, M. Lewenstein, and K. Rzazewski, *Phys. Rev. A* **28**, 2269 (1983).
- ¹⁹G. S. Agarwal, *Phys. Rev. Lett.* **37**, 1383 (1976); J. H. Eberly, *ibid.* **37**, 1387 (1976); B. J. Dalton and P. L. Knight, *J. Phys. B* **15**, 3997 (1982).
- ²⁰R. Loudon, *The Quantum Theory of Light*, 1st Ed. (Calderon, Oxford, 1978), p. 152.
- ²¹See, e.g., Ref. 2(b), Appendix A.
- ²²See also G. S. Agarwal, S. L. Haan, and J. Cooper, *Phys. Rev. A* **29**, 2552 (1984).
- ²³S. H. Autler and C. H. Townes, *Phys. Rev.* **100**, 703 (1955).
- ²⁴P. W. Milonni, private communication.